

Resonant slepton production at the LHC in models with an ultralight gravitino

B.C. Allanach^a, Manoranjan Guchait^b, K. Sridhar^b

^a*LAPTH, 9 Chemin de Bellevue, B.P. 110, Annecy-le-Vieux 74951, France*

^b*Tata Institute of Fundamental Research, Homi Bhabha Road, Mumbai 400 005, India*

Abstract

We examine resonant slepton production at the LHC with gravitinos in the final state. We examine the case when the slepton undergoes gauge decay into neutralino and a lepton, the neutralino decays into a photon and a gravitino. By measuring the transverse masses of the $\gamma\tilde{G}$ and the $l\gamma\tilde{G}$ subsystems it is possible to accurately reconstruct both the slepton and neutralino masses. In some regions of parameter space the slepton decays directly into a lepton and gravitino, giving an identical experimental topology to W production ($l\cancel{E}_T$). We present the novel matrix element squared for lepton-graviton production. A peak in the tail of the lepton-missing momentum transverse mass distribution of the W provides a signature for the process and an accurate measurement of the slepton mass. We display the search reach for the LHC and 300 fb^{-1} of integrated luminosity.

1 Introduction

This letter is devoted to the study of the signals at the Large Hadron Collider (LHC) due to a supersymmetric generalisation of the Standard Model (SM) which (a) violates R -parity, and (b) has an ultra-light gravitino in its spectrum. Despite the negative results that experimental searches for supersymmetric particles have yielded so far, the philosophy underlying these searches has been rather exclusive. The so-called minimal supergravity inspired R -conserving model of minimal supersymmetry or the constrained minimal supersymmetric standard model (CMSSM), as it is sometimes called, has been elevated to the status of a paradigm in the quest for supersymmetry at colliders. The adherence to this model to the exclusion of a myriad of other possibilities is not desirable. This is motivation enough to consider other models which relax some of the assumptions made in the CMSSM.

The quest to depart from the narrow confines of the CMSSM inexorably leads one to question the assumption of R -parity conservation as well as seeking alternatives to the mass spectrum of supersymmetric (SUSY) particles predicted by the minimal supergravity models. Of these two paths, the second is certainly more interesting, connected as it is with the fundamental issue of SUSY breaking. Of particular interest is the question of the lightest superparticle (LSP) because the decay patterns of the heavier particles into the LSP decide several of the collider search strategies for supersymmetry. In the preferred models, the LSP (most often the neutralino) is assumed to be in the mass range just above the reach of present experiments i.e. of $O(100)$ GeV in mass. All the other sparticles, are by definition, heavier than the LSP (the next-to lightest we denote the NLSP). A dramatic alternative is to have an ultralight gravitino as the LSP. The gravitino, in some models of supersymmetry breaking such as gauge-mediated supersymmetry breaking [6], can be as light as 10^{-3} eV: other sparticles then decay into the gravitino and this can significantly alter the strategies for supersymmetric particle searches at colliders. The other scenario wherein the LSP is not stable is that of R -parity violation where the decays of the neutralino yield final-states with jets, leptons or missing- E_T . But R -parity violation has another interesting implication, *ie* the sparticles can be produced singly. If this single sparticle production process proceeds via the s -channel, then the cross-section is resonantly enhanced and may be significant even for small values of the R -parity violating coupling.

An anomaly in the CDF experiment in the production rate of lepton-photon- \cancel{E}_T in $p\bar{p}$ collisions at $\sqrt{s} = 1.8$ TeV was observed using 86.34 pb^{-1} of Tevatron 1994-95 data [1]. While the number of events expected from the SM is 7.6 ± 0.7 , the experimentally measured number corresponded to 16. Moreover, 11 of these events involved muons (with 4.2 ± 0.5 expected) and 5 electrons (with 3.4 ± 0.3 expected). These anomalous events can be simply understood [2] in terms of a supersymmetric model with the following features: (1) the model is R -parity violating with an L -violating λ'_{211} coupling, and (2) the supersymmetric spectrum includes an ultra-light gravitino of mass $\sim 10^{-3}$ eV. The resonant production of a smuon via the R -violating coupling, its decay into neutralino and a muon and, finally, the decay of the neutralino into a gravitino and a photon leads to the $\mu\gamma\cancel{E}_T$ final state studied in the CDF experiment. The range of smuon and neutralino masses relevant to the explanation of these anomalous observations of the the CDF experiment is such that most of this range will be explored at the Run II of the Tevatron. In the event that this signal is not seen at Run II it will rule out the model at the lower end of the neutralino and smuon masses.

For heavier smuon and neutralino masses (above 250 GeV, roughly), the aforementioned Run I signal would be a statistical fluke and will probably disappear in Run II data. In that case, the LHC can be expected to discover and measure the sparticles. In this paper, we perform a study of the ability of the LHC to

perform these two tasks, identifying the sensitive observables.

2 The model

We assume throughout this paper that of all the R -violating couplings, only one lepton-number violating coupling is significantly large while the others are too small to have observable consequences. The coupling appears as

$$\lambda'_{ijk} L_i Q_j D_k \subset W \quad (1)$$

in the superpotential (where i, j, k are family indices, gauge indices have been suppressed and L_i , Q_j , D_k denote the left-handed lepton doublet, the left-handed quark doublet and the charge-conjugated right-handed down quark superfields respectively). This coupling allows for the production of a slepton from the initial state of quarks. The slepton thus produced could decay again via the R -violating coupling into two quarks. However, if the R -violating coupling is small, the existence of an ultralight gravitino in the mass range of 10^{-3} eV drastically alters the decay mode of the slepton. The slepton overwhelmingly decays into a lepton and a (bino-dominated) neutralino, with the latter decaying into a photon and a gravitino resulting in a $l\gamma\cancel{E}_T$ final-state. The Feynman diagram for the process is shown in Fig. 1. Since $m_{\tilde{\nu}} < m_{\tilde{\mu}_L}$ we should also expect signals from sneutrino production. In the case of sneutrino production, the process $q\bar{q}' \rightarrow \tilde{\nu} \rightarrow \gamma\tilde{G}\nu$ gives rise to a $\gamma\cancel{E}_T$ final-state. We will not study this final state in this paper, since the background depends crucially on cosmic ray events which are difficult to estimate. In our model, the only other light sparticles are the neutralino (which is lighter than the slepton) and the ultra-light gravitino (which is as light as 10^{-3} eV). We enforce degeneracy between the first two generations in order to avoid flavour changing neutral currents. Other sparticles do not play a role in this analysis, and are set to be arbitrarily heavy.

Such a light gravitino materialises naturally in models of gauge-mediated supersymmetry breaking (GMSB)[6]. However, in minimal GMSB models the chargino and the second-lightest neutralino are not much heavier than the neutralino. This is certainly not desirable for our considerations because it leads to large jets+ γ + \cancel{E}_T rates which are not seen by experiments¹. The question that naturally follows is how we can deviate from the minimal versions of GMSB models and obtain the pattern of supersymmetric masses that we require. It is interesting to note that such a mass spectrum can arise in an alternate model of GMSB which is obtained from compactifying 11-dimensional M-theory on a

¹ This observation has been made earlier in the literature [7] in the context of the GMSB-based explanation [8] of the $ee\gamma\gamma\cancel{E}_T$ CDF event [9].

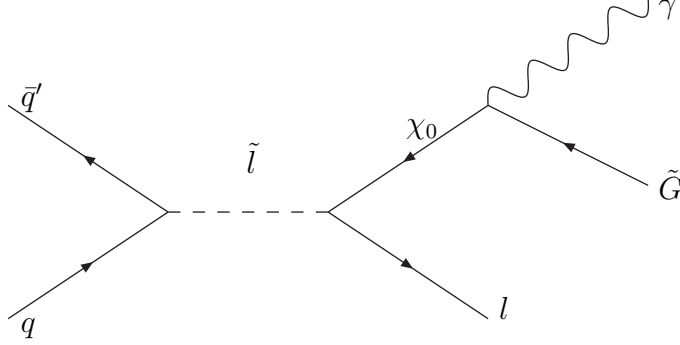


Fig. 1. Feynman diagram of resonant slepton production followed by neutralino decay.

7-manifold of G2 holonomy [10]. However, the detailed low-energy predictions of this model have not been worked out so for our analysis we simply work with the low-energy model described above.

3 Simulation Results

For our study of the process shown in Fig. 1 at the LHC (pp collisions at the $\sqrt{s} = 14$ TeV), we have chosen to work with the following default set of model parameters (unless indicated otherwise):

- Gravitino mass, $m_{\tilde{G}} = 10^{-3}$ eV,
- R -violating coupling $\lambda' \equiv \lambda'_{211} = 0.01$,
- $\tan\beta = 10$,
- sparticle masses $(m_{\chi_1^0}, m_{\tilde{l}}) = (120 \text{ GeV}, 200 \text{ GeV})$ or $(200 \text{ GeV}, 500 \text{ GeV})$ GeV (“low mass” and “high mass” scenarios) respectively.

The choice of using λ'_{211} rather than some other flavour combination is arbitrary. Our results can be easily generalised to other R -violating couplings and we will comment upon this below. Note that the chosen value of λ'_{211} is much smaller than the bound coming from $R_\pi = \Gamma(\pi \rightarrow e\nu)/(\pi \rightarrow \mu\nu)$ [11]: $\lambda'_{211} < 0.059 \times \frac{m_{\tilde{d}_R}}{100 \text{ GeV}}$ [12] even for a squark mass of 100 GeV. However, since the squark mass is arbitrarily large in our model, this constraint is not relevant to our analysis. The R -violating decay of the slepton is possible but constrained, in principle, by the Tevatron di-jet data [13] which exclude a $\sigma.B > 1.3 \times 10^4$ pb at 95% C.L. for a resonance mass of 200 GeV. However, in practice this does not provide a restrictive bound upon our scenario as long as the R -violating coupling is sufficiently small, $< \mathcal{O}(1)$. Moreover, the di-jet bound is not restrictive because it suffers from a huge QCD background. By

restricting λ'_{211} and the gravitino mass to be small, we avoid significant rates for the possible R -violating decays of $\chi_1^0 \rightarrow \mu jj$ or $\chi_1^0 \rightarrow \nu jj$. $\chi_1^- \rightarrow \gamma \tilde{G}$ is the dominant channel.

We use the **ISASUSY** part of the **ISAJET7.58** package [14] to generate the spectrum, branching ratios and decays of the sparticles. For an example of parameters, we choose (in the notation used by ref. [14]) $\tan \beta = 10$ and $A_{t,\tau,b} = 0$. μ together with other flavour diagonal soft supersymmetry breaking parameters are set to be very large. We emphasise that this is a representative point in the supersymmetric parameter space and not a special choice.

3.1 Slepton decays to lepton, photon and gravitino

The signal has been simulated using **HERWIG6.4** [15]. The $W\gamma$ SM background to the $\mu\gamma\cancel{E}_T$ and $\gamma\cancel{E}_T$ channels have been simulated using **PYTHIA** [16]. Because the background took a restrictively long time to calculate, 10 times *less* background luminosity was simulated than signal luminosity. The background has then been scaled up by a factor of 10 for all results presented here, but it should be borne in mind that the statistical fluctuations within it are bigger than will be expected. For our simulations of the signal and the background we have used only selection cuts of $E_T > 25$ GeV on the transverse energies of the muon and the photon. The same cut of 25 GeV is also used for \cancel{E}_T . We have used the following cuts on the rapidity of the photon and the muon: $|\eta_{\gamma,\mu}| < 3$. There is an isolation cut between the photon and other hard objects o in the event of $\sqrt{(\eta_\gamma - \eta_o)^2 + (\phi_\gamma - \phi_o)^2} > 0.7$. Since the signal is hadronically quiet, we veto events with jets reconstructed with $E_T > 30$ GeV and $\eta_j < 4$. Initial and final state radiation effects, as well as fragmentation effects are included in the background simulation.

The E_T distributions of γ, μ and \cancel{E}_T in the simulated events are shown in Figs. 2 (a)-(c). It would be very difficult to claim a signal for the low or high mass scenarios based on these distributions, given uncertainties involved in the background calculation. However, the figures illustrate the fact that the signal to background ratio could be improved by tightening the E_T cuts, to 50 GeV for example. We leave the optimisation of cuts to a future, more detailed study.

The transverse mass distributions of several particles i

$$M_T = \sqrt{(\sum_i E_T^i)^2 - (\sum_i \underline{p}_T^i)^2} \quad (2)$$

should possess a sharp peak at the mass of the particle which decays to i daugh-

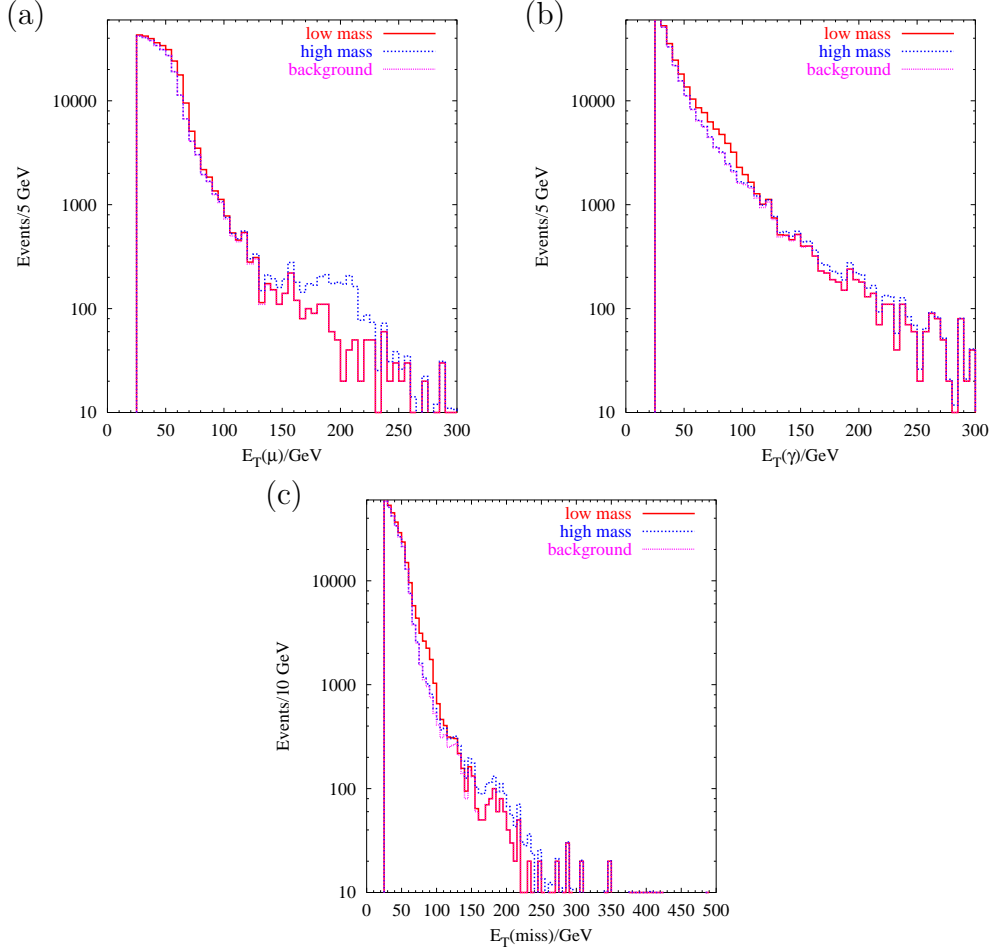


Fig. 2. E_T distributions of (a) muons, (b) photons and (c) missing- E_T for $\mu\gamma\cancel{E}_T$ events that pass the cuts. 300 fb^{-1} integrated luminosity at the LHC is assumed. The purple (lighter) histograms display $W\gamma$ SM background, the red (darker) histograms show the signal plus background for $(m_{\chi_1^0}, m_{\tilde{l}}) = (120 \text{ GeV}, 200 \text{ GeV})$, whereas the blue (dotted) histograms display the signal plus background distributions for $(m_{\chi_1^0}, m_{\tilde{l}}) = (200 \text{ GeV}, 500 \text{ GeV})$.

ters. The $M_T(\mu\gamma\cancel{E}_T)$ and $M_T(\gamma\cancel{E}_T)$ distributions are displayed in Figs. 3a,b for the simulated high and low mass points and $W\gamma$ simulated SM background. In Fig. 3a, sharp peaks in the $M_T(\mu\gamma\cancel{E}_T)$ are clearly visible at values of the smuon mass and will be detected above the SM $W\gamma$ background. The smuon mass could be accurately measured in this manner. The background gives a negligible number of events above $M_T(\mu\gamma\cancel{E}_T) > 450 \text{ GeV}$. Fig. 3b shows that the signal peaks in $M_T(\gamma\cancel{E}_T)$ (predicted to be at the neutralino mass) should be able to provide a measurement of the neutralino mass.

In order to calculate the search reach, we use the signal S in the 4 highest peak bins (covering 20 GeV) of $M_T(\mu\gamma\cancel{E}_T)$. The background distribution in these four bins is estimated by fitting a simple function to $M_T(\gamma\mu\cancel{E}_T)$ between

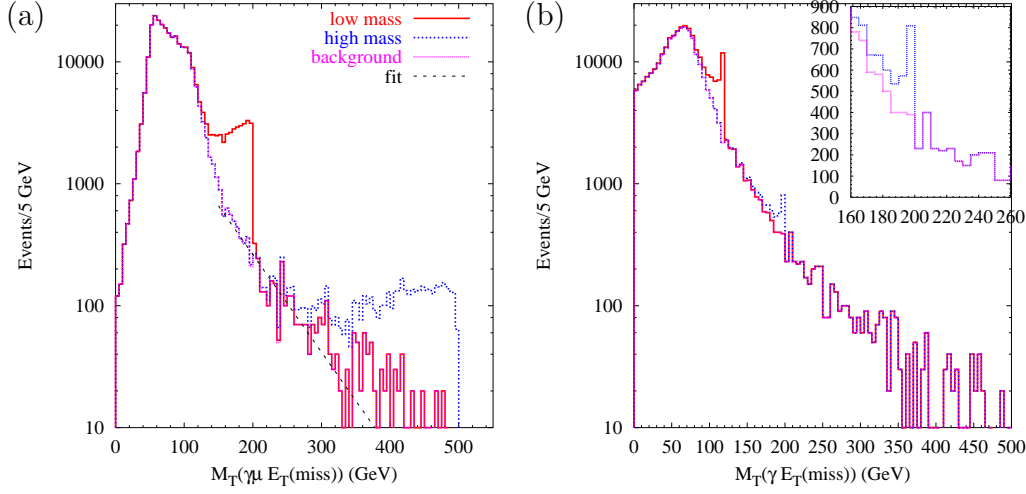


Fig. 3. M_T distributions of (a) $\mu\gamma E_T$, (b) γE_T for slepton. 300 fb^{-1} integrated luminosity at the LHC is assumed. The purple (lighter) histograms display $W\gamma$ SM background, the red (darker) histograms show signal plus background for $(m_{\chi_1^0}, m_{\tilde{l}}) = (120 \text{ GeV}, 200 \text{ GeV})$, whereas the blue (dotted) histograms display the signal plus background distributions for $(m_{\chi_1^0}, m_{\tilde{l}}) = (200 \text{ GeV}, 500 \text{ GeV})$. In (a), the dashed black line displays a log-linear fit to the background distribution for $M_T = 150 - 400$ GeV. In (b), the insert shows a linear scale magnification of an area of the plot.

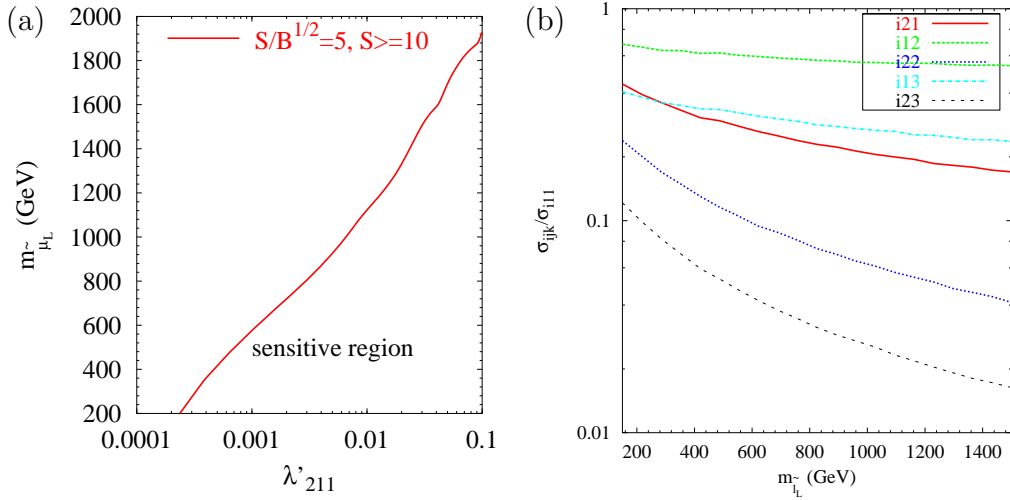


Fig. 4. (a) Search reach for the $\mu\gamma E_T$ signal (as defined in the text) for 300 fb^{-1} integrated luminosity at the LHC. (b) Relative production cross-sections for the different flavour choices of λ'_{ijk} couplings as a function of the slepton mass.

150-400 GeV in Fig. 3a. We use

$$B = 4\exp[aM_T(\mu\gamma E_T) + b] \quad (3)$$

with purely \sqrt{B} statistical errors, leading to $a = -0.018 \pm 0.001$, $b = 9.25 \pm 0.22$. B is displayed in Fig. 3a as the dashed black line. We define the sensitive region of parameter space to be any region for which² $S/\sqrt{B} > 5$ and $S \geq 10$. For 300 fb^{-1} , the search reach is shown as a function of smuon mass and R-parity conserving coupling in Fig. 4a for the case of a neutralino NLSP.

If a different R-parity violating (RPV) flavour coupling than λ'_{211} was used, the analysis would be much the same provided the coupling did not involve taus or top quarks. The main difference would be that, for a given size of RPV coupling, the production cross-section would decrease because one no longer probes valence partons in the proton. Fig. 4b shows that the suppression of the cross-section also depends upon the slepton mass, since different regions of x are being probed in the parton distributions. For a fixed slepton mass, the ratio of production cross sections $\sigma(\lambda_{ijk} = c)/\sigma(\lambda_{i11} = c)$ is shown. The parton distributions of top quarks are not known, so we do not include the possibility that the RPV coupling involves the top (λ'_{i3j}). The figure shows that the production cross-section can decrease to less than 10% of its original value by changing the flavour structure of the RPV coupling to include heavy quarks. The number of produced events for different flavours of RPV coupling other than λ'_{211} can therefore be determined by multiplying the ratio of cross sections in Fig. 4b with the number of events in Fig. 4a. One must then ask how the number of *measured* signal events depends upon the lepton flavour of the RPV coupling used. Efficiencies and backgrounds for the e and μ case will differ somewhat depending upon the experiment, and so changing the lepton flavour involved in the RPV coupling could quantitatively affect the result. τ reconstruction efficiencies are significantly different to those of e, μ and so there would be a large change in number of measured events in that case.

There is no particular need to rely on a neutralino NLSP. Indeed, recent studies have found sleptons to be lighter than neutralinos in, for example, large regions of RPV mSUGRA space [17]. Later (for a different final state), we will consider the possibility of a smuon NLSP, and contrast it with the neutralino NLSP case.

3.2 Slepton decays to gravitino and lepton

We now turn to the decay $\tilde{l} \rightarrow \tilde{G}l$. We ignore sneutrino production in this case because it would lead to an invisible final state. Neglecting lepton masses, the partial widths for the decays of \tilde{l} [6,11] are

² The statistical uncertainties on fitted a and b parameters make a negligible difference to the final numerical results.

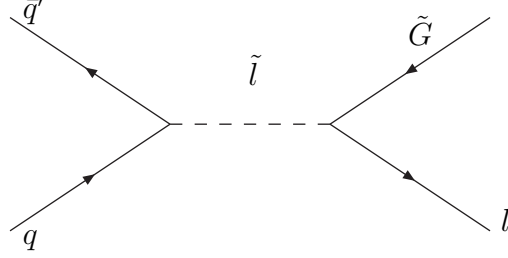


Fig. 5. Feynman diagram of resonant slepton production followed by decay into a lepton and gravitino

$$\begin{aligned}\Gamma(\tilde{l} \rightarrow \tilde{G}l) &= \frac{m_{\tilde{l}}^5}{48\pi M_P^2 m_{\tilde{G}}^2}, & \Gamma(\tilde{l} \rightarrow q\bar{q}') &= \frac{3\lambda'^2 m_{\tilde{l}}}{16\pi} \\ \Gamma(\tilde{l} \rightarrow l\chi_1^0) &= |b|^2 \frac{m_{\chi_1^0}}{8\pi} \left[\frac{m_{\chi_1^0}}{m_{\tilde{\mu}}} \left(1 - \left(\frac{m_{\chi_1^0}}{m_{\tilde{\mu}}} \right)^2 \right)^2 \right],\end{aligned}\quad (4)$$

where $b = eN_{11} + gN_{12}(1/2 - \sin^2\theta_w)/\cos\theta_w$ and N_{ij} denote neutralino mixing matrix elements [20]. $\Gamma(\tilde{l} \rightarrow \tilde{G}l)$ thus dominates for large $m_{\tilde{l}}$ and small $m_{\tilde{G}}$.

The Feynman diagram of the process in question is displayed in Fig. 5 and we calculate the spin and colour averaged matrix element squared to be:

$$|\bar{M}|^2 = \frac{\lambda'^2 m_{\tilde{l}}^4}{36 M_P^2 m_{\tilde{G}}^2} \frac{s^2}{(s - m_{\tilde{l}})^2 + \Gamma^2 m_{\tilde{l}}^2}, \quad (5)$$

where s is the centre-of-mass energy of the colliding $q\bar{q}'$ system, $M_P = 2.4 \times 10^{18}$ GeV is the reduced Planck mass and Γ is the total decay width of the slepton.

This new process is not simulated in HERWIG, so we perform the phase space integration by the method of Monte-Carlo integration ourselves. For this reason, the simulation was not of generated events and is therefore not subject to associated statistical errors. We have use cuts on the muon and missing transverse energy identical to the $\gamma\mu\cancel{E}_T$ analysis, i.e. $\cancel{E}_T, E_T^\mu > 25$ GeV and $|\eta_\mu| < 3$.

The $M_T(\mu\cancel{E}_T)$ distribution is displayed in Fig. 6a for the SM W background plus signal in two cases: $m_{\tilde{\mu}} = 1.2$ TeV, 1.5 TeV. If we use the default value of $\lambda'_{211} = 0.01$ and the neutralino is the NLSP, we obtain the smaller peaks which would not be prominent enough to claim a 5σ discovery. If the smuon is the NLSP, the decay mode to neutralinos is not open, leading to a higher

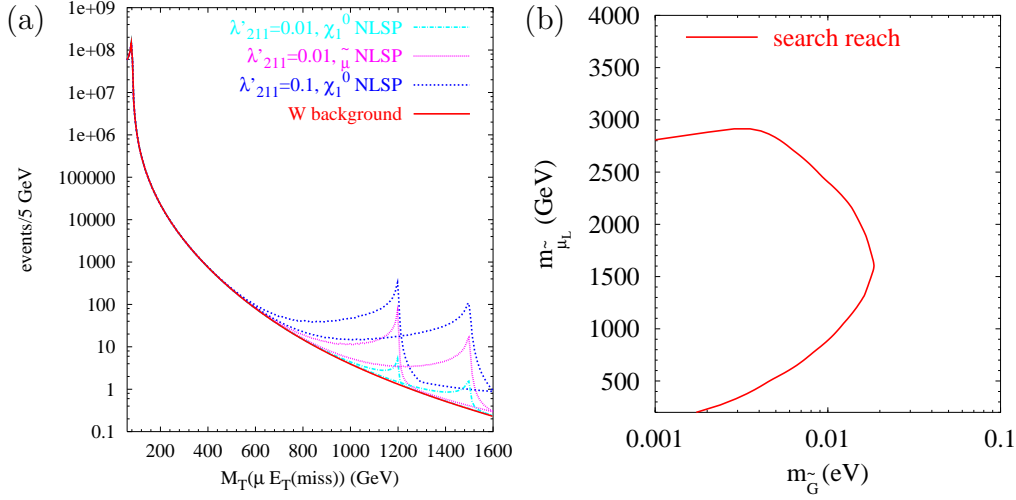


Fig. 6. (a) M_T distribution of the $\mu\tilde{G}$ final state for two different values of the smuon mass and 300 fb^{-1} integrated luminosity at the LHC. The left(right)-most three peaks are for smuon masses of 1.2 and 1.5 TeV respectively. (b) Search reach (as defined in the text) for the $\mu\tilde{G}$ final state, a *neutralino* NLSP and 300 fb^{-1} integrated luminosity at the LHC and $\lambda'_{211} = 0.1$. The search reach is contained to the left of the curve.

branching ratio for $\tilde{\mu} \rightarrow \tilde{G}\mu$. The magenta (middle height) curves in Fig. 6a are evidence for this, and should be observable even for the small value of $\lambda'_{211} = 0.01$. The signal cross section scales as $\lambda'_{211}{}^2$, and for $\lambda'_{211} = 0.1$ we obtain the one-hundred times larger peaks, either of which would be easy to detect on top of the SM W background, even for a neutralino NLSP.

In this subsection, we define the search reach by the criteria that for S signal and B background events, $S/\sqrt{B} \geq 5$ and $S \geq 10$ in the 5 GeV signal peak bin of $M_T(\mu\cancel{E}_T)$. These constraints lead to the expected search reach for 300 fb^{-1} luminosity shown in Fig. 6b for a neutralino NLSP. For smuon masses that are too low, the huge background swamps the signal in the peak bin. For smuon masses that are too high, the signal production cross-section is too low. The search region is shown as the region to the left of the curve in Fig. 6b.

As explained above, it is easier to detect the $\mu\tilde{G}$ final state if the smuon is the NLSP, because the relevant branching ratio is larger. Thus we expect a larger region of sensitivity. The search reach in two different planes of parameter space are displayed in Fig. 7 for the case of a smuon NLSP. For $\lambda'_{211} = 0.1$, the region of sensitivity is modestly larger than the neutralino NLSP case, as can be seen by comparing the blue curve in Fig. 7 with the one in Fig. 6b. However, there is no possibility searching for a peak with $\lambda'_{211} = 0.01$ with a neutralino NLSP, whereas a smuon NLSP is still detectable up to $m_{\tilde{\mu}} \approx 1500 \text{ GeV}$, as displayed in Fig. 7a.

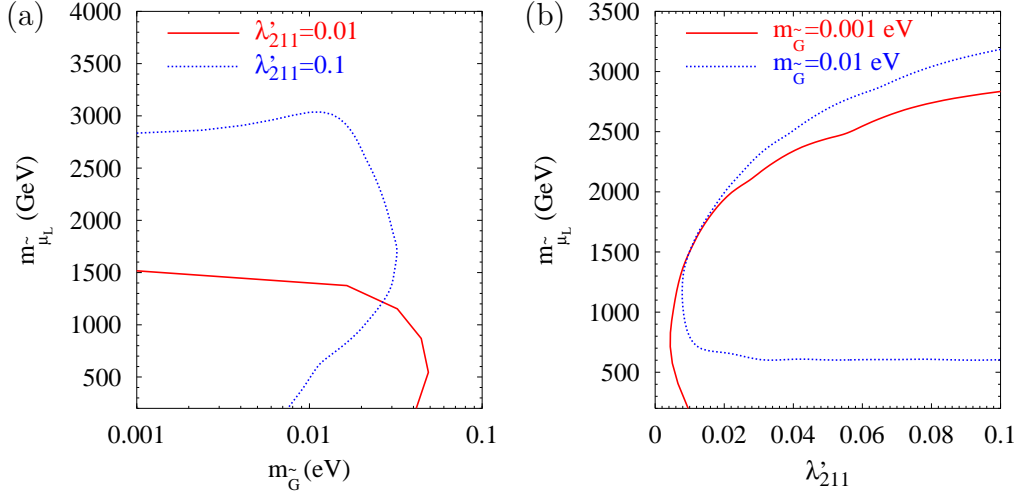


Fig. 7. Region of sensitivity to the $M_T(\mu\tilde{G})$ peak for 300 fb^{-1} at the LHC for a *smuon* NLSP. The region of sensitivity is (a) to the left hand side of the curves, (b) to the right hand side of the curves.

4 Conclusions

We have provided a basic first study of the search for resonant slepton production at the LHC with ultra light gravitinos in the final state. We have not performed a detailed detector simulation, with associated mis-tagged backgrounds, \cancel{E}_T resolution and detection efficiencies. We started with a simple and loose set of cuts, and provided distributions which indicate how signal to background ratio can be improved. Specific cases of RPV coupling and other parameters are taken in order to be concrete, but the analysis applies over a wide range of parameter space.

The current paper shows which are the sensitive variables (various M_T distributions are the most useful) and displays the rough search reach one can expect. Luckily, signal peaks in M_T distributions mean that one does not have to know the backgrounds very well. The backgrounds can be measured and fitted away from the peaks, whereas the position of the peak provides an accurate measurement of the slepton mass. Although detector efficiencies and non-physics backgrounds will erode the search reach somewhat, it could be possible to flavour subtract some backgrounds. SM background processes from $W \rightarrow l\nu$ are lepton-flavour universal. On the other hand, if one RPV coupling is dominant over others, the signal only contributes to the production of one lepton flavour. Thus, subtracting the number of electron-tagged events from the number of muon-tagged events would greatly improve the signal to background ratio. The only pitfall of this approach is that it is possible that two RPV couplings are of similar strengths and therefore one could cancel any signal. Although this only happens in a very limited region of parameter

space, one cannot *a priori* rule this pessimistic scenario out and so we have not included it in our analysis. The process $q\bar{q}' \rightarrow \tilde{l} \rightarrow \tilde{G}l$ has not been studied before, and we presented the matrix element squared together with the search reach and M_T distributions.

We have concentrated on LHC studies, but of course the same $\tilde{\mu} \rightarrow \mu\tilde{G}$ production analysis could be applied to the Tevatron, with lighter smuons than those considered here. The important indicator would still be a peak in the $M_T(\mu)$ tail, above M_W . Instead of smuon production, we could instead have considered squark production through a baryon-number violating coupling $1/2\lambda''_{ijk}U_iD_jD_k$ in the superpotential. We would then have signals of $j\gamma\cancel{E}_T$ in the neutralino NLSP case³ and $j\cancel{E}_T$ (“monojet” signature). The sensitivity of the Tevatron and LHC to these processes is presumably less than in the slepton-production case, but remains to be calculated. In that case, the same M_T variables will be appropriate for detection, but some of the cuts may need to be harder in order to beat down a larger background.

Acknowledgements

This work was conceived and commenced at the Les Houches workshop *Physics at Tev colliders*. We would like to thank Giacomo Polesello for discussions and helpful comments during the Les Houches workshop. K Sridhar would like to thank LAPTH for hospitality offered while part of this work was carried out.

References

- [1] D. Acosta et al, Phys. Rev. D66 (2002) 012004, hep-ex/0110015; D. Acosta et al, Phys. Rev. Lett. 89 (2002) 041802, hep-ex/0202044.
- [2] B.C. Allanach and K. Sridhar, Phys. Lett. B551 (2003) 343, hep-ph/0210375; B.C. Allanach, S. Lola and K. Sridhar, Phys. Rev. Lett. 89 (2002) 011801, hep-ph/0111014; B.C. Allanach, S. Lola and K. Sridhar, JHEP 0204 (2002) 002, hep-ph/0112321.
- [3] S. Abachi et al, Phys. Rev. Lett. 78 (1997) 3634, hep-ex/9612002.
- [4] D. Acosta et al, hep-ex/0205057; T. Fahland, Ph. D. thesis (1997) Brown University, can be viewed at URL http://www-d0.fnal.gov/results/publications_talks/thesis/fahland/thesis.ps
- [5] B.C. Allanach, Comput. Phys. Comm. 143 (2002) 305, hep-ph/0104145.

³ j denotes a hard jet

- [6] G. Giudice and R. Rattazzi, Phys. Rept. 322 (1999) 419 and references therein.
- [7] H. Baer, M. Brhlik, C. Chen and X. Tata, Phys. Rev. D55 (1997) 4463.
- [8] S. Ambrosanio, G. L. Kane, G. D. Kribs, S. P. Martin, and S. Mrenna, Phys. Rev. Lett. 76 (1996) 3498; G. L. Kane and S. Mrenna, Phys. Rev. Lett. 77 (1996) 3502; S. Ambrosanio, G. L. Kane, G. D. Kribs, S. P. Martin, and S. Mrenna, Phys. Rev. D55 (1997) 1372.
- [9] F. Abe et al, Phys. Rev. D59 (1999) 092002.
- [10] E. Witten, hep-ph/0201018 and talk at SUSY 2002, can be viewed at URL <http://www.desy.de/~susy02/pl.6/witten.pdf>
- [11] V. Barger, G. F. Giudice and T. Han, Phys. Rev. D 40 (1989) 2987.
- [12] B. C. Allanach, A. Dedes, and H. K. Dreiner, Phys. Rev. D60, 075014 (1999), hep-ph/9906209; H. Dreiner, ‘Perspectives on Supersymmetry’, Ed. by G.L. Kane, World Scientific.
- [13] F. Abe et al, Phys. Rev. D55 (1997) 5263.
- [14] F. E. Paige, S. D. Protopescu, H. Baer and X. Tata, hep-ph/9810440.
- [15] G. Corcella et al, hep-ph/0201201; G. Marchesini, B. R. Webber, G. Abbiendi, I. G. Knowles, M. H. Seymour and L. Stanco, JHEP 01 (2001) 010 hep-ph/0011363; *ibid.* hep-ph/0107071. G. Marchesini et al, Comput. Phys. Commun. 67 (1992) 465.
- [16] T. Sjostrand, L. Lonnblad, S. Mrenna and P. Skands, arXiv:hep-ph/0308153.
- [17] B. C. Allanach, A. Dedes and H. K. Dreiner, arXiv:hep-ph/0309196.
- [18] F. James and M. Roos, Comput. Phys. Commun. 10 (1975) 343.
- [19] LEPSUSYWG, ALEPH, DELPHI, L3 and OPAL experiments, note LEPSUSYWG/02-07.1 <http://lepsusy.web.cern.ch/lepsusy/Welcome.html>
- [20] Peter Richardson, PhD thesis, hep-ph/0101105